Influence of particle size and temperature on the dielectric properties of $CoFe_2O_4$ nanoparticles

Deepshikha Rathore[1], Rajnish Kurchania[2], and R. K. Pandey[1]

1) NIIT University, Neemrana-301705 (Raj.), India

2) Department of Physics, Maulana Azad National Institute of Technology (MANIT), Bhopal-462051 (M.P.), India

Abstract: The objective of this study was to establish the dielectric properties of $CoFe_2O_4$ nanoparticles with particle sizes that varied from 28.6 to 5.8 nm. $CoFe_2O_4$ nanoparticles were synthesized using a chemical coprecipitation method. The particle sizes were calculated according to the Scherrer formula using X-ray diffraction (XRD) peaks, and the particle size distribution curves were constructed by using field-emission scanning electron microscopy (FESEM) images. The dielectric permittivity and loss tangents of the samples were determined in the frequency range of 1 kHz to 1 MHz and in the temperature range of 300 to 10 K. Both the dielectric permittivity and the loss tangent were found to decrease with increasing frequency and decreasing temperature. For the smallest $CoFe_2O_4$ nanoparticle size, the dielectric permittivity and loss tangent exhibited their highest and lowest values, respectively. This behavior is very useful for materials used in devices that operate in the microwave or radio frequency ranges.

1. Introduction

The AB_2X_4 spinels represent one of the most attractive and significant families of crystalline compounds, where A, B, and X denote a divalent cation, a trivalent cation, and a divalent anion, respectively [1]. Cobalt ferrite ($CoFe_2O_4$) nanoparticles are of great interest because of their size-dependent dielectric properties that vary with frequency and operating temperature [2]. The dielectric permittivity [3] and dissipation factor ($tan\delta$) [4] are two basic parameters used to determine the dielectric properties of $CoFe_2O_4$ nanoparticles. These parameters depend on three fundamental factors: (1) ionic and dipolar relaxation, (2) atomic vibration, and (3) electronic resonance at high frequencies. Ionic and dipolar relaxation is most dominant among these three factors [5]. Ferrites, which are very good dielectric materials, have numerous applications in microwave-frequency- and radio-frequency-range devices [6] because they exhibit very low electrical conductivity [7]. They are therefore used as an essential ingredient in electromagnetic devices that operate in the microwave frequency range. The

microwave behavior can be significantly modified through the application of a biasing field [8]. Because of their high resistivity, ferrites can also be used as high-frequency magnetic materials [9].

In high-frequency applications [10], understanding of the dielectric properties of materials is very important. The dielectric properties of $CoFe_2O_4$ nanoparticles depend upon the technique used to synthesize them [11]. In recent years, numerous synthesis procedures for synthesizing nanoscale ferrites have been developed. The synthesis of ferrites using a chemical coprecipitation [12] method has many advantages over other wet chemical methods. These advantages include maximum reactivity, short processing time, low preparation temperature, homogenous distribution of ions, and low costs [13].

In this study, $CoFe_2O_4$ nanoparticles with different sizes have been synthesized by a chemical coprecipitation method at different temperatures from 75 to 10°C and different molar fractions to establish the dependence of their dielectric properties on their particle size without using any surfactant. To the best of our knowledge, this method has not been re-

🙢 Springer

ported previously. Controlled synthesis without using any surfactant may increase the possibility of preparing highly pure, single-crystalline nanoferrites.

2. Experimental

CoFe₂O₄ nanoparticles were synthesized via a chemical coprecipitation method. The reagents CoCl₂·6H₂O (Merck, 99.9% pure) and FeCl₃·6H₂O (S.D. Fine Chem, 99.9% pure) were mixed in an aqueous solution in a Co/Fe molar ratio of 1:2. An aqueous solution with an excess of NaOH was used as the alkaline precipitating agent. The reaction temperatures were constantly maintained at the desired temperature from 10 to 75°C, and the molar fractions of the reagents were varied with each set of samples, as shown in Fig. 1. Sets I, II, and III were synthesized at FeCl₃·6H₂O/ CoCl₂·6H₂O/NaOH molar ratio of 2:1:16 and at molar fractions of 1%, 5%, and 10%, respectively. Specimens (a), (b), (c), and (d) were synthesized at 10, 25, 55, and 75°C, respectively. We synthesized a series of nanoparticle samples by controlling the dilution of the precursors while keeping the molar ratios constant. When the mixed solution was dripped into the alkaline aqueous solution, precipitation occurred immediately and the color of the suspension changed from the initially brown to dark-brown over a period of 2 h. The reaction time of 2 h was found to be sufficient for the dehydration and atomic rearrangement involved in the conversion of the hydroxide into the ferrite compound. The magnetic separation technique was used to separate the magnetic particles from the solution using a 0.1 T magnetic field; the magnetic particles were subsequently washed five times with distilled water to remove sodium and chloride ions. The washed samples were dried at room temperature and calcined at 200°C for 2 h.

The structural properties of CoFe₂O₄ nanoparticles were characterized by powder X-ray diffraction (XRD) (Bruker diffractometer, model D8 Advance) using Cu K$_\alpha$ radiation in the range 20°–80°; the scan rate was 0.02°/s, and the X-ray source was operated at 40 kV and 40 mA. Surface morphological and microstructural properties were investigated using atomic force microscopy (AFM) (M/s Digital Instruments, model NSE) and field emission scanning electron microscopy (FESEM) (JEOL JSM-6390A). The dielectric properties were measured using an HP 4284A Precision LCR meter in the frequency range of 100 kHz to 1 MHz at low temperature using a model CCS-150 liquid-helium cryostat (Janis Research Company, USA). The temperature of the device was controlled using a Lakeshore model 331 temperature controller and a GaAlAs temperature sensor.
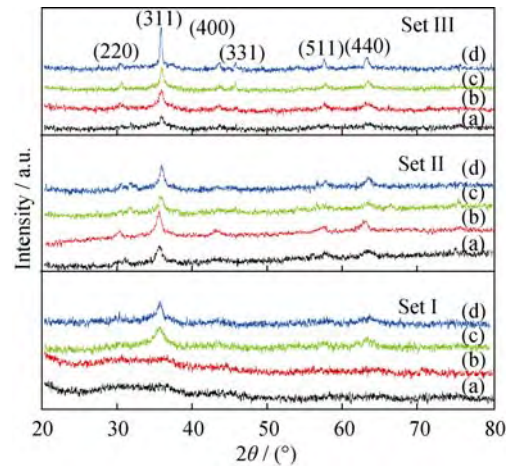

Fig. 1. XRD patterns of CoFe₂O₄ nanoparticles synthesized at different temperatures using various molar fractions of reagents. Set I, set II, and set III were synthesized at molar fractions of 1%, 5%, and 10% respectively. (a), (b), (c), and (d) were synthesized at 10, 25, 55, and 75°C, respectively.

3. Results and discussion

3.1. Structural properties

The XRD patterns of CoFe₂O₄ nanoparticles synthesized at different temperatures and molar fractions are shown in Fig. 1. Analysis of the XRD patterns revealed that all samples consisted of CoFe₂O₄ (JCPDS No. 00-022-1086), had a single-phase cubic structure, and contained no other phases/impurities. The particle sizes were determined using the Scherrer formula [14]:

$$t = \frac{0.89\lambda}{\beta\cos\theta} \tag{1}$$

where β is the full-width at half-maximum (FWHM) corrected for instrument-induced line broadening using silicon as a standard sample, λ is the wavelength of the X-rays, and θ is the Bragg angle.

As shown in Fig. 1, the samples in sets I (a) and (b) are amorphous because of the low molar fraction and low reaction temperatures. The average particle sizes are 5.8 and 9.2 nm for sets I (c) and (d), respectively, 10.2, 10.7, 11.8, and 13.6 nm for sets II (a), (b), (c), and (d), respectively, and 14.4, 16.2, 17.3, and 28.6 nm for sets III (a), (b), (c), and (d), respectively.

The average particle sizes and the assigned structure are tabulated in Table 1 for the different sets of molar fractions and temperatures used in the experiments. The XRD results show that the sharpness of the prominent peak increases with increasing reaction temperature and molar fraction of the reagents, which indicates that the grain size increased, as seen in Fig. 1 and Table 1. This result can also be understood with the help of the Debye–Scherrer formula because

410

Int. J. Miner. Metall. Mater., Vol. 21, No. 4, Apr. 2014

the particle size is inversely proportional to β (FWHM). Cedeño-Mattei *et al.* [15] have also reported that the sharpness of the prominent peak increases as the grain size of nanomaterials increases.

Table 1. Summary of the growth process variables, grain sizes, and phase assignments for sample sets I, II, and III

Set	Molar fraction / %	Temperature / °C	Grain size / nm	Phase assignment
I	1	10	—	Amorphous
		25	—	Amorphous
		55	5.8	Cubic
		75	9.2	Cubic
II	5	10	10.2	Cubic
		25	10.7	Cubic
		55	11.8	Cubic
		75	13.6	Cubic
III	10	10	14.4	Cubic
		25	16.2	Cubic
		55	17.3	Cubic
		75	28.6	Cubic

3.2. Dielectric properties

The dielectric properties of the $CoFe_2O_4$ nanoparticles of various sizes were studied in the temperature range from 300 to 10 K at different frequencies using an LCR (HP 4284A) meter, a liquid-helium cryostat, and a temperature controller. Nanoparticles of $CoFe_2O_4$ were pressed using a uniaxial press into pellets with a diameter of 10 mm and a thickness of 0.1 mm. Silver paste was applied to both sides of the pellet to form a metal–insulator–metal parallel-plate capacitor configuration. The dielectric permittivity [16] was calculated using Eq. (2):

$$\varepsilon_r = \frac{Cd}{\varepsilon_0 A} \tag{2}$$

where ε_r is the dielectric permittivity of the sample, C is the capacitance of the sample, d is the thickness of the sample, $\varepsilon_0 = 8.854 \times 10^{-12}$ F/m is the permittivity of free space, and A is the cross-sectional area of the sample.

The dielectric permittivity of $CoFe_2O_4$ nanoparticles as a function of temperature at frequencies of 1 kHz and 1 MHz and for particle sizes that ranged from 28.6 to 5.8 nm is shown in Fig. 2. As evident in Fig. 2, the dielectric permittivity increases as the particle size decreases from 28.6 to 5.8 nm. The enhancement of the dielectric properties as the particle size decreases can be explained by the correlated barrier hopping (CBH) model [17]. For the CBH model,

ions or charge carriers are assumed to be separated by a potential well (or anisotropy barrier) and to jump from one site to another site over the barrier. When the particle size decreases to 5.8 nm, the number of domains decreases and the particles remain single-domain. A weak field is required to overcome the barrier and results in an enhancement of the dielectric permittivity [18].

Results in Fig. 2 also indicate that, as the temperature decreases from 300 to 175 K, the dielectric permittivity decreases very rapidly due to the rearrangement of dipoles in the direction of the electric field. Furthermore, at lower temperatures from 175 to 10 K, the $CoFe_2O_4$ nanoparticles exhibit almost constant dielectric permittivity values because of an anisotropy barrier that prevents the polarization direction of each nanoparticle from flipping at low temperatures [19]. At low temperatures, dipoles are frozen and exhibit a low degree of polarization; as a result, the dielectric permittivity does not significantly change.

Variation of the dielectric permittivity as a function of frequency for different particle sizes of $CoFe_2O_4$ nanoparticles at 300 and 175 K is shown in Fig. 3. Figs. 2 and 3 clearly indicate that the dielectric permittivity at a frequency of 1 kHz is greater than that at a frequency of 1 MHz for all particle sizes. As the frequency increased from 200 kHz to 1 MHz, the $CoFe_2O_4$ nanoparticles exhibited almost constant values of dielectric permittivity.

Dielectric polarization occurs as electronic, ionic, interfacial, or dipolar polarization. Electronic and ionic polarizations are active in the high-frequency range, whereas the other two mechanisms prevail in the low-frequency range [20]. When the frequency is increased, the dipoles will no longer be able to rotate sufficiently fast, and their oscillations will begin to lag behind that of the field. As the frequency is further increased, the dipole will be completely unable to follow the field and the orientation polarization will stop. Consequently, the dielectric permittivity decreases at higher frequencies and approaches a constant value. This behavior is believed to be due to the vanished interfacial or space charge polarization [20].

Fig. 4 illustrates $\tan\delta$ as a function of frequency at different temperatures of $CoFe_2O_4$ nanoparticles with different particle sizes. As evident in Fig. 4, as the particle size is reduced from 28.6 nm to 5.8 nm, $\tan\delta$ also decreases due to the superparamagnetic behavior of the smallest particles [19]. We also observed that the $\tan\delta$ gradually decreases as the frequency increases to 1 MHz and also decreases as the temperature decreases from 300 to 175 K [20]. At temperatures less than 175 K, $CoFe_2O_4$ nanoparticles adopt constant values of $\tan\delta$ because the anisotropy barrier prevents the polarization direction of each nanoparticle from flipping [19].
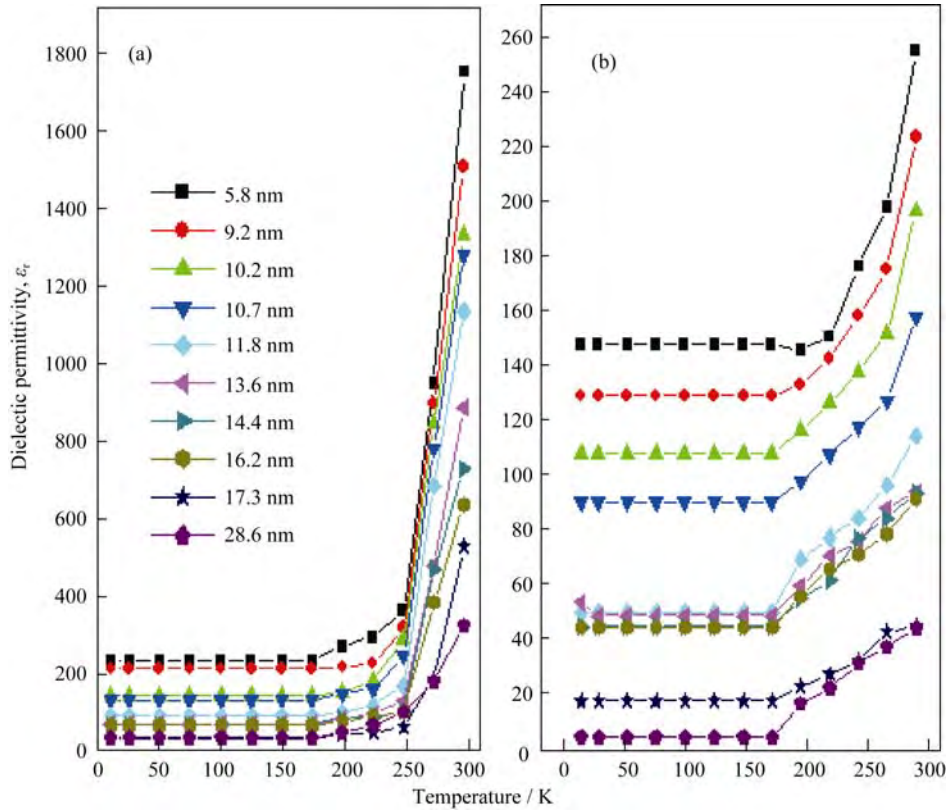
Fig. 2. **Dielectric permittivity as a function of temperature at frequencies of 1 kHz (a) and 1 MHz (b) for all sizes of CoFe$_2$O$_4$ nanoparticles.**
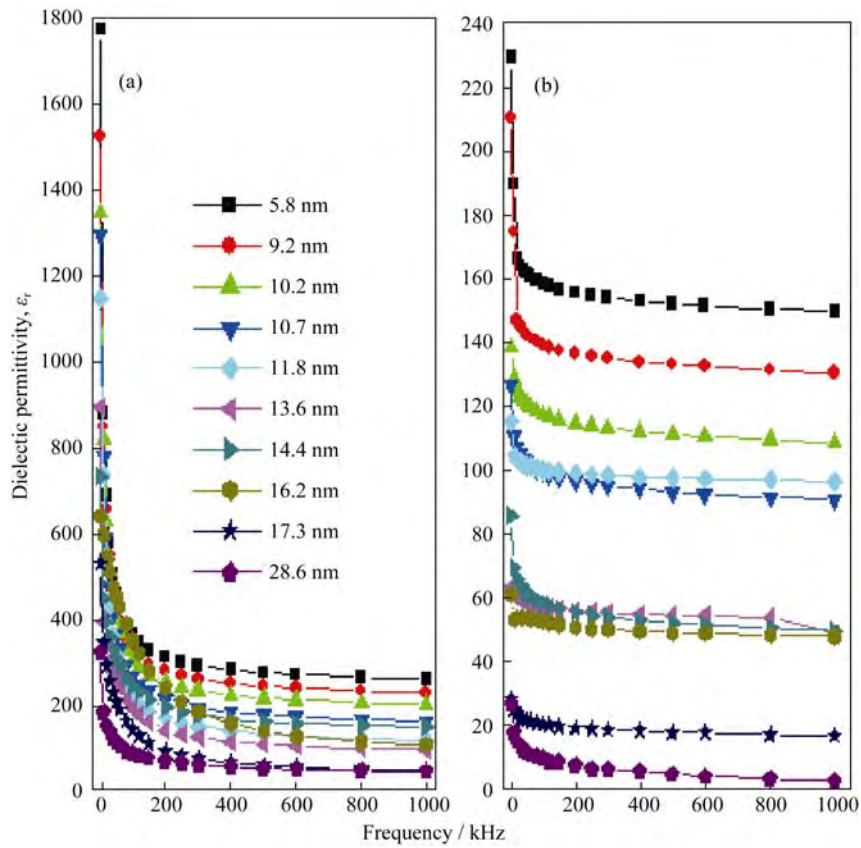

Fig. 3. **Variation of the dielectric permittivity with frequency for different particle sizes of CoFe$_2$O$_4$ nanoparticles at 300 K (a) and 175 K (b).**
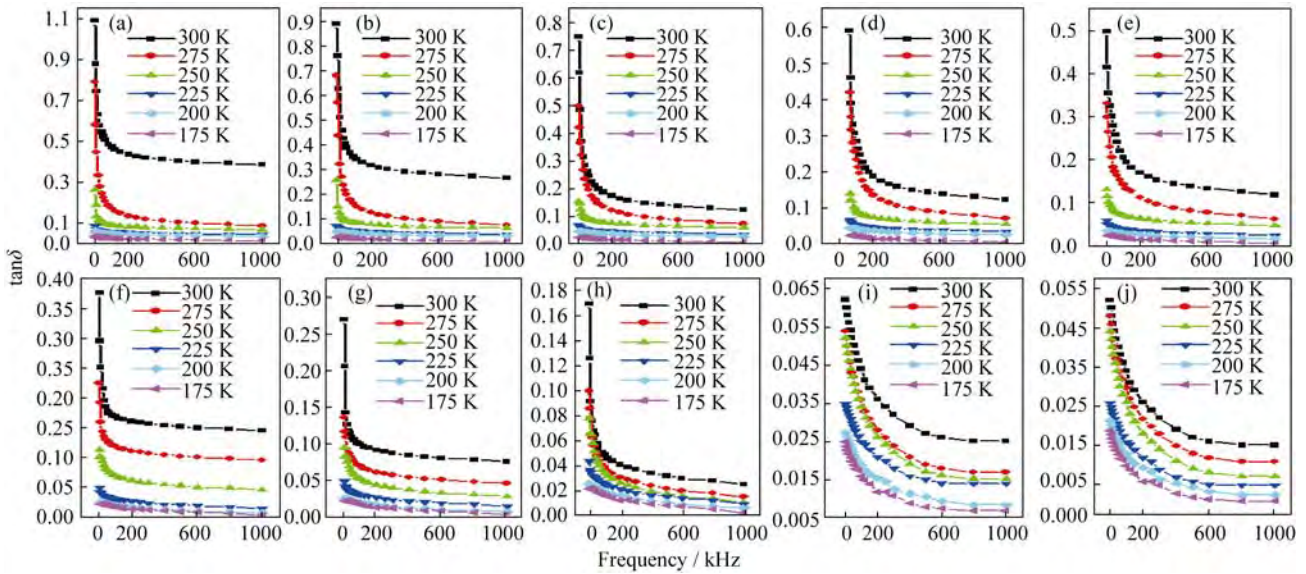
Fig. 4. Loss tangent (tanδ) as a function of frequency at different temperatures of CoFe$_2$O$_4$ nanoparticles corresponding to the particle sizes of 28.6 nm (a), 17.3 nm (b), 16.2 nm (c), 14.4 nm (d), 13.6 nm (e), 11.8 nm (f), 10.7 nm (g), 10.2 nm (h), 9.2 nm (i), and 5.8 nm (j).

In general, tanδ is a measure of the loss-rate of energy of a mode of oscillation (mechanical, electrical, or electrome-chanical) in a dissipative system. It is the reciprocal of the quality factor, which represents the quality of oscillation. Electrical potential energy is dissipated in all dielectric ma-terials, usually in the form of heat [21]. An ideal capacitor exhibits a small dissipation factor [22]. The previously men-tioned results indicate that a capacitor device fabricated from the 5.8-nm CoFe$_2$O$_4$ nanoparticles can be considered as an ideal capacitor.

3.3. Surface morphology

Surface morphological investigations were performed using field-emission scanning electron microscopy (FESEM) measurements. Characteristic FESEM results related to the morphological properties of the ultrafine dispersion of CoFe$_2$O$_4$ nanoparticles corresponding to particle sizes 5.8 and 28.6 nm are shown in Fig. 5 along with the high-resolution images. Both the samples of CoFe$_2$O$_4$ nanoparticles exhibit a homo-

geneous, cubic nanocrystalline morphology. The particle size distribution and its Gaussian fit are illustrated in Figs. 6(a) and 6(b) for the 5.8 nm and 28.6 nm CoFe$_2$O$_4$ nanopar-ticles, respectively. The size distribution curves clearly show that the majority of cubic nanocrystallites have a particle size close to (a) 5.8 nm or (b) 28.6 nm with a dispersion of (a) $\pm$ 2 and (b) $\pm$ 3 nm, which confirms that our XRD and FE-SEM analysis results are in good agreement with each other.

4. Conclusions

(1) Our results show that the synthesis of highly crystal-line, ultrafine, and pure particles of cubic-phase CoFe$_2$O$_4$ using Fe and Co chloride as precursors and sodium hydrox-ide as a precipitant was successful. The reaction temperature and molar fraction of reagents were found to be two very important parameters in the synthesis of highly pure CoFe$_2$O$_4$ nanoparticles by a chemical coprecipitation method that did not involve the use of a surfactant.
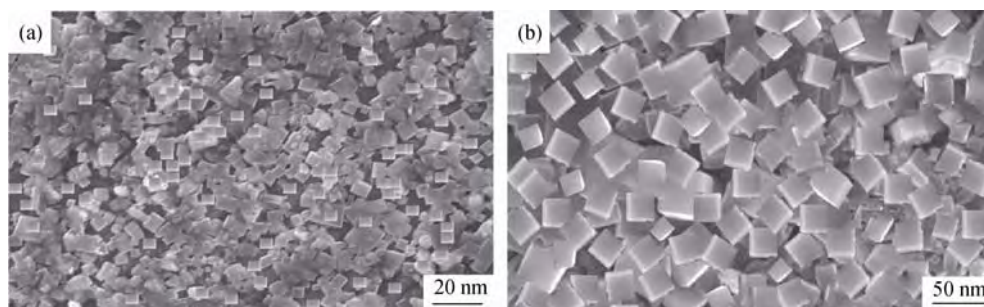

Fig. 5. Typical FESEM images of CoFe$_2$O$_4$ nanoparticles with sizes of 5.8 nm (a) and 28.6 nm (b).
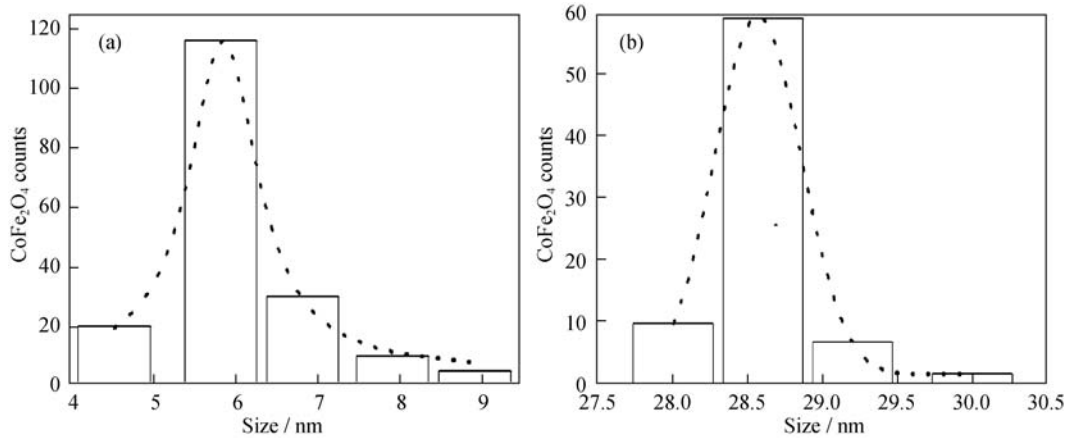
Fig. 6.   Particle size distribution of CoFe₂O₄ nanoparticles corresponding to average particle sizes of 5.8 nm (a) and 28.6 nm (b).

(2) The dielectric permittivity of $CoFe_2O_4$ nanoparticles rapidly decreases as the temperature decreases from 300 to 175 K and achieves almost constant values at lower temperatures of 175 to 10 K due to an anisotropy barrier. The dielectric permittivity decreases gradually as the frequency increases and becomes constant at high frequencies due to the disappearance of interfacial or space charge polarization. The loss tangent slowly decreases as the frequency increases up to 1 MHz and the temperature decreases up to 175 K. The dielectric permittivity increases as the grain size decreases and reaches its maximum value in the case of 5.8-nm particles, whereas the loss tangent decreases as the grain size decreases and reaches its smallest value in the case of 5.8-nm particles. These features are very important for devices that operate in the microwave or radio frequency range.

(3) The XRD results show that the $CoFe_2O_4$ nanoparticles are cubic; this result was confirmed by the nanoparticles' surface morphological and microstructural properties. The XRD and FESEM analysis results agree well with each other.

Acknowledgements

References

[1]   Y.H. Hou, Y.J. Zhao, Z.W. Liu, H.Y. Yu, X.C. Zhong, W.Q. Qiu, D.C. Zeng, and L.S. Wen, Structural, electronic and magnetic properties of partially inverse spinel CoFe₂O₄: a first-principles study, *J. Phys. D*, 43(2010), No. 44, art. No. 445003.

[2]   S.C. Watawe, B.D. Sarwade, S.S. Bellad, B.D. Sutar, and B.K. Chougule, Microstructure, frequency and temperature-dependent dielectric properties of cobalt-substituted lithium ferrites, *J. Magn. Magn. Mater.*, 214(2000), No. 1-2, p. 55.

[3]   A.M. Bhavikatti, S. Kuikarni, and A. Lagashetty, Evaluation of AC conductivity & dielectric behavior of cobalt ferrite, *Int. J. Eng. Sci. Technol.*, 3(2011), No. 7, p. 5985.

[4]   S.F. Mansour, Frequency and composition dependence on the dielectric properties for Mg–Zn ferrite, *Egypt. J. Solids*, 28(2005), No. 2, p. 263.

[5]   E. Barsoukov and J.R. Macdonald, *Impedance Spectroscopy: Theory, Experiment, and Applications*, *Migration in the Absence of Concentration Gradients*, I.D. Raistrick, D.R. Franceschetti, and J.R. Macdonald, eds., John Wiley & Sons, Inc., Hoboken, New Jersey, 2005, p. 47.

[6]   A.T. Raghavender and K.M. Jadhav, Dielectric properties of Al-substituted Co ferrite nanoparticles, *Bull. Mater. Sci.*, 32(2009), No. 6, p. 575.

[7]   G. Ranga Mohan, D. Ravinder, A.V. Ramana Reddy, and B.S. Boyanov, Dielectric properties of polycrystalline mixed nickel–zinc ferrites, *Mater. Let.*, 40(1999), No. 1, p. 39.

[8]   E. Schlömann, Behavior of ferrites in the microwave frequency range, *J. Phys. Colloq.*, 32(1971), p. C1-443.

[9]   S. Son, M. Taheri, E. Carpenter, V.G. Harris, and M.E. McHenry, Synthesis of ferrite and nickel ferrite nanoparticles using radio-frequency thermal plasma torch, *J. Appl. Phys.*, 91(2002), No. 10, p. 7589.

[10]   D. Ravinder, K.V. Kumar, and P. Balaya, High-frequency dielectric behaviour of gadolinium substituted Ni–Zn ferrites, *Mater. Lett.* 48(2001), No. 3-4, p. 210.

[11]   X. Shen, Y.X. Wang, X. Yang, Y. Xia, J.F. Zhuang, and P.D. Tang, Megahertz magneto-dielectric properties of nanosized NiZnCo ferrite from CTAB-assisted hydrothermal process, *Trans. Nanoferrous Met. Soc. China*, 19(2009), No. 6, p. 1588.

[12]   K. Maaz, A. Mumtaz, S.K. Hasanain, and A. Ceylan, Synthesis and magnetic properties of cobalt ferrite (CoFe₂O₄) nanoparticles prepared by wet chemical route, *J. Magn. Magn.*

Mater., 308(2007), No. 2, p. 289.

[13] T.M. Meaz, M.A. Amer, and M.K. El-Nimr, Studies of magnetic structure of cobalt-ferrite nano-particles, *Egypt. J. Solids*, 31(2008), No. 1, p. 147.

[14] B.D. Cullity, *Element of X-ray Diffraction*, M. Cohen, ed., Addison-Wesley, London, 1978, p. 102.

[15] Y. Cedeño-Mattei, O. Perales-Perez, M.S. Tomar, F. Roman, P.M. Voyles, and W.G. Stratton, Tuning of magnetic properties in cobalt ferrite nanocrystals, *J. Appl. Phys.*, 103(2008), art. No. 07E512.

[16] R.P. Mahajan, K.K. Patankar, M.B. Kothale, and S.A. Patil, Conductivity, dielectric behaviour and magnetoelectric effect in copper ferrite–barium titanate composites, *Bull. Mater. Sci.*, 23(2000), No. 4, p. 273.

[17] D. Rathore, R. Kurchania, and R.K. Pandey, Structural, magnetic and dielectric properties of $Ni_{1-x}Zn_xFe_2O_4$ ($x = 0$, 0.5 and 1) nanoparticles synthesized by chemical co-precipitation method, *J. Nanosci. Nanotech.*, 13(2013), p.

1812.

[18] M. George, S.S. Nair, K.A. Malini, P.A. Joy, and M.R. Anantharaman, Finite size effects on the electrical properties of sol–gel synthesized $CoFe_2O_4$ powders: deviation from Maxwell–Wagner theory and evidence of surface polarization effects, *J. Phys. D,* 40(2007), No. 6, p. 1593.

[19] C. Liu, A.J. Rondinone, and Z.J. Zhang, Synthesis of magnetic spinel ferrite $CoFe_2O_4$ nanoparticles from ferric salt and characterization of the size-dependent superparamagnetic properties, *Pure Appl. Chem.*, 72(2000), No. 1-2, p. 37.

[20] A.A. Hendi, AC conductivity and dielectric measurements of bulk tertracyanoquinodimethane, *Aust. J. Bas. Appl. Sci.*, 5(2011), No. 7, p. 380.

[21] B.W. Griffith, *Radio-Electronic Transmission Fundamentals*, 2nd Ed., SciTech Publishing, 2000, p. 41.

[22] S. Salivahanan, N. S. Kumar, and A. Vallavaraj, *Electronic Devices and Circuits*, 7th Ed., Tata McGraw-Hill Pune, 1998, p. 36.